Journal of Materials Processing Technology 225 (2015) 337–346

Contents lists available at ScienceDirect

Journal of Materials Processing Technology

journal homepage: www.elsevier.com/locate/jmatprotec

# Diamond micro engraving of gravure roller mould for roll-to-roll printing of fine line electronics

XinQuan Zhang*, Kui Liu, Vasudivan Sunappan, Xuechuan Shan

*Singapore Institute of Manufacturing Technology, 71 Nanyang Drive, 638075, Singapore*

ARTICLE INFO

*Article history:*
Received 20 October 2014
Received in revised form 5 May 2015
Accepted 20 May 2015
Available online 24 June 2015

*Keywords:*
Ultraprecision diamond machining
Slow slide servo
Roll-to-Roll gravure printing
Metal mesh film

ABSTRACT

Printing electronics has attracted great attention in recent years due to its various superior performances compared with conventional silicon-based semiconductor industry. Roll-to-Roll gravure printing is able to transfer conductive nanoparticle ink onto the flexible film substrate to form continuous fine metal lines using a gravure roller mould with tens of thousands of tiny gravure cells on its surface. However, it is difficult to scale down the printed line width, which is crucial for the film's circuit density, resolution and transparency, because the market-available rollers fabricated by conventional engraving techniques for graphic printing usually have gravure cells larger than 25 μm. Hence, in this study, a novel method based on ultraprecision machining technology, Diamond Micro Engraving (DME), is introduced to miniaturize the gravure cells in order to reduce the ink volume transfer during the printing process. A V-shape sharp diamond tool is used to continuously generate concave inverted micro pyramidal structures on the gravure roller surface using the Slow Slide Servo technology. Geometrical modelling of the engraving process is conducted to help programming the tool path to realize accurate control of the instantaneous position of two linear axes and one rotatory axis. Through applying the DME process, generation of consistent cell structure is achieved. The engraved gravure cell width is successfully miniaturized to 7 μm. With the optimized cell spacing value, the DME-machined roller moulds are used in gravure printing of metal mesh film, which works as a potential transparent conductive film to replace the expensive indium-tin-oxide (ITO). The printed line width is reduced from 47 μm to 19 μm, and the transmittance of the printed metal mesh film for visible light is increased from 65.2% to 80.4% accordingly, which is comparable to the transmittance of ITO film.



## 1. Introduction

Recently, printing electronics has received significant attention because of its low manufacturing cost per unit area, light weight, and high flexibility compared to conventional silicon-based semiconductor electronics. It provides a better alternative to realize low-cost and high-volume manufacturing of a wide range of flexible and costless electronic systems, such as radio-frequency identification tags (RFID), electronics labels, sensors, and transparent conductive films. There are a number of attempts by researchers to realize printing electronics using various methods, such as inkjet printing, screen printing, flexographic printing, offset printing, pad printing, and Roll-to-Roll (R2R) gravure printing. Compared to the other printing methods, R2R gravure printing has the advantages of excellent pattern fidelity, homogeneous thickness of printed layer, high throughput due to high printing speed, high printing resolution. Pudas et al. (2005) firstly applied R2R gravure printing technique to transfer conductive inks onto flexible substrates to form conductive lines on paper and plastic films. Then, Sung et al. (2010) has used R2R gravure printing to realize the scaling of printed conductive line width down to 30 μm. Hrehorova et al. (2011) also successfully applied gravure printing of electronics on glass, which is more common but rigid.

Gravure printing was widely used in high-quality graphic printing (e.g. fine art, bank notes, magazines, postage stamps, and photography reproduction) due to its remarkable density range since the late of 19th century. Colour intensities of the printed feature are directly determined by the amount of ink transferred onto the substrates. Typically, the size of printed features of gravure printing is larger than 50 μm. Miniaturization of cell size is not necessary in paper printing industry because it will exceed the capability of human vision with naked eyes. However, for printing of high-performance electronics, Kang et al. (2012) has found that scaling down of the printed features is essential because

* Corresponding author.
*E-mail address:* zhangxq@simtech.a-star.edu.sg (X. Zhang).

http://dx.doi.org/10.1016/j.jmatprotec.2015.05.032

**Nomenclature**

| | |
|---|---|
| $h$ | Height of gravure cell |
| $w$ | Width of gravure cell |
| $\theta$ | Tool included angle |
| $\alpha$ | Effective rake angle |
| $\alpha_{in}$ | Instantaneous effective rake angle during cut-in session |
| $\alpha_{out}$ | Instantaneous effective rake angle during cut-out session |
| $\delta$ | Tool clearance angle |
| $\varphi$ | Rhombus interior angle |
| $\gamma_{in}$ | Tool cut-in angle during DME |
| $\gamma_{out}$ | Tool cut-out angle during DME |
| $V_c$ | Cell volume |

smaller printed features will provide higher circuit density, higher transition frequency of transistors and lower operating voltages. Gravure printing of electronics employs a high-precision gravure roller mould to transfer conductive nanoparticle ink onto flexible substrates using engraved gravure cells on the roller, and the ink volume transferred onto the substrate is directly determined by the volume of engraved cells. Sung et al. (2010) has found that the printed line width is about 2–3 times larger than the gravure cell width, and scaling down of the gravure cell size is the most straightforward way to reduce the size of printed features. This will require a high-precision gravure cylinder with smaller cell size and consistent cell structure.

Traditionally, three major engraving technologies are widely used in paper printing industry: 1) laser engraving, 2) chemical etching, and 3) electro-mechanical engraving. In laser engraving process, a laser beam is focused onto the gravure cylinder surface coated with a zinc layer to create cells. Each laser pulse creates one cell, and its cell width, depth and volume are determined by beam size and energy of the pulse. In chemical etching, laser ablation is also applied by indirectly machining the specified area to be engraved, prior to the chemical etching process. As the chemically etching usually has identical material removal rate, the cell volume is usually altered by the varying cell width and etching time. Electro-mechanical engraving is the most widely used engraving method nowadays. A high-frequency oscillating diamond tip is used to engrave gravure cells as cylinder rotates, and one oscillation produces one single cell. The cell width, depth and volume are changed by applying different oscillation amplitudes and tool geometries.

A common limitation of the three conventional engraving techniques is that the engraved cell size is usually larger than 25 $\mu$m, and this is resulted from the large spot size of laser beam, the inaccurate engraving machine system, the material removing mechanism, and so on. More importantly, conventional engraving methods also suffer from non-uniform gravure pattern due to the lack of environmental temperature control, low positioning and repositioning accuracy, external and internal vibration, and inconsistent etching rate, etc. Although this resulted micron-level inaccuracy of cell/pattern does not affect the performance in gravure printing of decorative papers, it could pose detrimental effects on the high-resolution electronics printing. For example, an abnormally large cell size may cause transferred ink spreading away and result in short circuit; and an unusually small cell size may cause unconnected electronic lines and result in open circuit. Although researchers (Kitsomboonloha et al., 2012) have recently applied photolithography to generate micro gravure cells on a small area with the cell size down to 1 $\mu$m, it is not possible to apply such technique to generate a large-area gravure pattern on rollers because it is very costly and time consuming.

Ultraprecision machining is an advanced material removal technology, which is introduced for machining various optics-related components in the late of 1950s. In 1983, Donaldson and Patterson (1983) reported the completion of the world's most precise machining system, Large Optics Diamond Turning Machine (LODTM), which is constructed by Lawrence Livermore National Laboratory. An ultraprecision machining system could provide high axis motion accuracy, minimum drifting of tool/workpiece position, nanometer movement resolution, and accurate control of tool path and instantaneous tool position. Ultraprecision diamond machining has been widely used in generation of mirror quality surface and sub-micron profile accuracy of workpieces made of many engineering materials through conventional machining processes such as turning, milling or fly cutting. But machining of microstructures with discontinuous concave structure is not possible with such conventional processes, as they usually rely on rotation for generating the required cutting motion. Recently, Brinksmeier et al. (2012a,b), Brinksmeier and Schönemann (2014) proposed a novel ultraprecision machining process, Diamond Micro Chiseling (DMC), to cut out each facet of a prismatic concave structure individually by redefining the tool geometry and finely designing the tool path. Their technology has demonstrated the potential of ultraprecision machining in generating arrays of discontinuous optical microstructures for the applications of cube corner retroreflectors.

In this study, another novel method, Diamond Micro Engraving (DME), is developed to realize miniaturization of gravure cells on high-precision gravure roller moulds for R2R printing of fine line electronics. Micro engraving is realized using a V-shape sharp diamond tool with customized geometrical shape to continuously generate concave inverted pyramid structures on the roller surface using an ultra-precision machining system. Based on geometrical modelling of the DME process, CNC tool path program is generated taking into account all the relevant parameters regarding the gravure pattern, cell, tool, and roller. During the engraving process, Slow Slide Servo technique is utilized to accurately control the position of two linear axes and one rotatory axis. By employing DME, gravure rollers with consistent sub-10 $\mu$m cells are successfully fabricated and are also applied in R2R gravure printing of metal mesh as a kind of transparent conductive film. Sub-20 $\mu$m printed line width is achieved, and transmittance of the printed metal mesh film has been increased to 80% accordingly.

## 2. Diamond micro engraving (DME)

### 2.1. Gravure pattern for printing metal mesh

In recent years, due to the rapid growth of smartphones, tablets and other electrical devices with touch panels, touch screen modules are obtaining wider and wider application around the world. Transparent conductive film (TCF) is a critical component in the touch screen modules, and until now, classic indium-tin-oxide (ITO) film is still the most widely used TCF in the industry. However, Indium, as the film's primary metal, is a rare earth material with limited reserves and its price is getting higher and higher due to high market demand, researchers are continuously looking for the alternatives of ITO, such as transparent organic conductors, silver nanowire, carbon nanotube, grapheme, and metal mesh. But each of these alternatives has their own limitation which is difficult to overcome, and none of them has found successful practical industry application until now.

Metal mesh is a promising alternative which has high potential to replace ITO, as it provides sufficient transparency and low

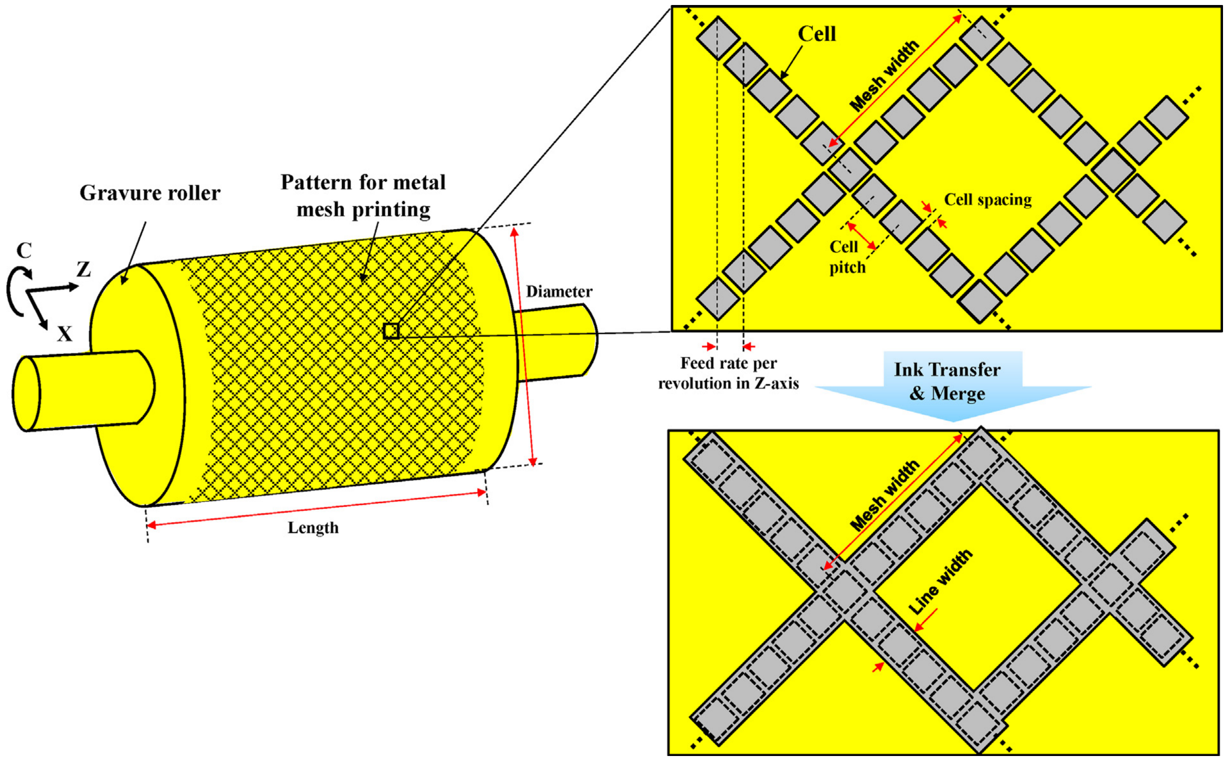


**Fig. 1.** Gravure roller with a specified pattern for metal mesh printing.

sheet resistance. Tvingstedt and Inganäs (2007) firstly demonstrated the possibility of replacing ITO with a set of thin conducting metal stripes which was generated using lithography metal deposition. To generate metal mesh on the flexible film, R2R gravure printing works as an effective, low-cost and high-throughput technique to transfer the nanoparticle conductive ink onto the film and form conductive metal lines after the ink merges. In order to print continuous metal lines of consistent line width without ragged edges, the gravure cell cavity should have a square shape on the top surface of the concave structure. Fig. 1 shows a gravure roller and its specifications of pattern and cell for metal mesh printing.

### 2.2. DME process

The general idea of DME is to use a V-shape sharp diamond tool to remove material from the roller surface with a single step of cutting motion, and to produce a gravure cell with a concave inverted pyramid microstructure. Continuous engraving of the cell pattern is realized by rotating the roller to the required angular position with $C$-axis and positioning the tool with the linear axes of $X$ and $Z$ (see Fig. 2). The concave cell structure is designed to have a square-shape top surface with an equal cell width of $w$ and a structure height of $h$. For obtaining such a structure, the bisecting line of the V-shape diamond tool should be set to be perpendicular to $Z$-axis, which is achieved by adjusting the $B$-axis assisted with an optical inspection system. Precise control of interactive movement of the tool and the roller using the Slow Slide Servo technique ensures the structural consistency and the dimensional accuracy of the consecutive gravure cells.

Geometrical design of the diamond tool is determined by the structure and dimensions of the engraved gravure cells. The diamond tool is customized to have a sharp nose (<1 μm) in order to engrave a structure with sharp edges and corners. To generate gravure cells with desired dimensions as illustrated in Fig. 2, the tool included angle $\theta$ is calculated as follows:

$$\theta = 2 \times \tan^{-1} \frac{w \times \sin\varphi/2 \times \cos\alpha}{h} \tag{1}$$

where $\alpha$ is the effective tool rake angle relative to the roller surface, and $\varphi$ is the interior angle of the rhombus surface of the inverted pyramid structure. In this study, the effective tool rake angle is preset to be zero, to simplify the tool path programming for generation of square-shape top surface.

In designing the tool path for cutting an inverted pyramid structure, assuming the effective rake angle is zero, the cut-in and cut-out angles, $\gamma_{in}$ and $\gamma_{out}$, should be set equal in order to ensure the generation of a top surface with an equal width $w$ ($\gamma_{in} = \gamma_{out}$, see Fig. 2). In that case, the rhombus interior angle, $\varphi$, can be calculated as follows:

$$\varphi = 2 \times \cos^{-1} \frac{h}{w \times \tan\gamma_{in}} \tag{2}$$

In gravure printing of electronics, square-shape top surface of the cell structure is desired to produce consistent printed metal line width without ragged edges. Hence, the interior angle should be set as 90°, and the cut-in/out angle can be calculated from the following equation:

$$\gamma_{in} = \gamma_{out} = \frac{180^o - \theta}{2} \tag{3}$$

During the cut-in and cut-out session in machining a single cell, the instantaneous effective rake angle will change accordingly due to the variation of tool velocity with respect of the roller surface. Fig. 3 shows section views of the DME process. It can be seen that the instantaneous rake angle in cut-in session ($\alpha_{in}$) is positive, while the rake angle in cut-out session ($\alpha_{out}$) is negative. Their values can be derived as follows:

$$\alpha_{in} = \gamma_{in} \tag{4}$$

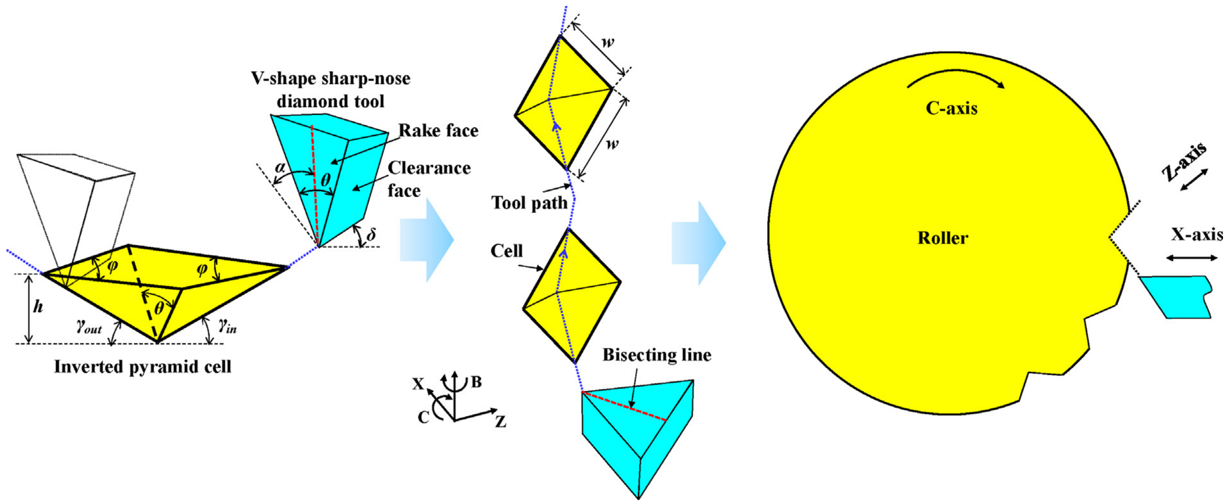


**Fig. 2.** DME process kinematics and relevant parameters for cutting concave inverted pyramid cells on a gravure roller mould.

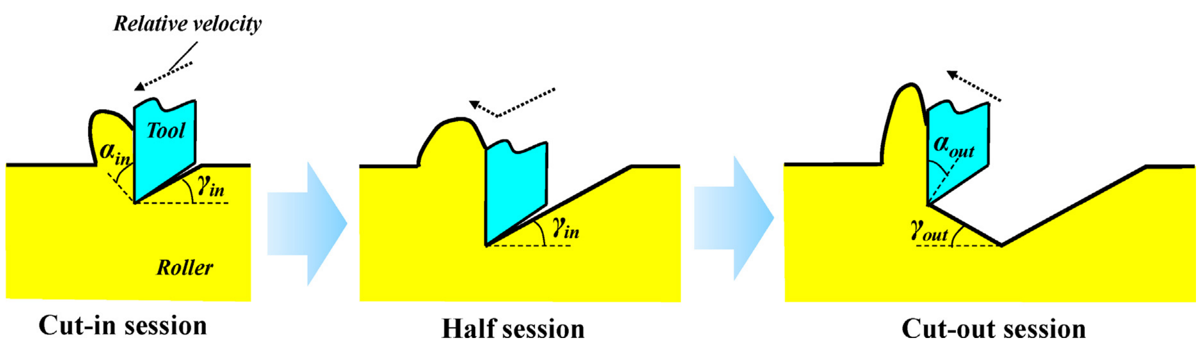


**Fig. 3.** Section views of DME process in machining a single cell.

$$\alpha_{\text{out}} = -\gamma_{\text{out}} \tag{5}$$

The tool clearance angle, $\delta$, is another important tool parameter affecting the generation of desired engraved cells. Although its value does not directly determine geometrical parameters of the inverted pyramid structure, an unsuitable clearance angle will lead to either a fragile tool nose\(for a too large clearance angle\) or the interference between the machined surface and the tool clearance face\(for a too small clearance angle\). Fig. 4 schematically shows the effects of different tool clearance angle in the proposed diamond micro engraving process. If the tool clearance angle is smaller than the cut-in angle ($\delta < \gamma_{\text{in}}$, see Fig. 4(a)), a non-square quadrilateral shape of the top cell surface will be generated, and unexpected burrs will be generated because metal materials are squeezed out of the cell cavity by the tool clearance faces. In contrast, if the clearance angle meets the requirement of $\delta < \gamma_{\text{in}}$, no interference between the tool clearance faces and the machined cell cavity will happen, and square-shape cell with burr-free edges and sharp corners can be generated on the roller surface.

## 3. Ultraprecision machining of gravure pattern by DME

### 3.1. DME using ultraprecision machining system

In this study, a 5-axis ultraprecision machine system (*Moore Nanotech 350FG*) is utilized to realize DME of the above gravure pattern which is composed of tens of thousands of cells on a metal roller mould. The ultraprecision machining system has a resolution of 1 nm for its three linear axes, and a resolution of 0.00001° for its *B* and *C* rotation axes. A cylinder made of brass is used as the raw roller, which is held on the vacuum chuck. A sharp diamond tool for DME and another round diamond tool with 1 mm nose radius for outer diameter turning of roller before engraving are held by two different tool holders on the *B*-stage, with their effective rake and swiveling angles measured and adjusted using an optical inspection system. A monitoring camera focusing on the tool cutting edge is used to assist setting the tool location and monitoring the DME process. Mist coolant is provided to blow away the generated chips during machining. In order to maintain consistent structure and size of the engraved cells, the air temperature inside the machine enclosure is controlled within ±0.1 °C using an air shower system to minimize thermal drifting of the machining system during the long-time machining period. Fig. 5 shows physical views of the 5-axis ultra-precision machine system and the experimental setup.

Firstly, based on the required cell structure composing the gravure pattern, geometrical parameters (included and clearance angles) of the V-shape diamond tool is calculated and customized. Then the CNC tool path for the DME process is generated considering the specified gravure pattern, cell structure and dimensions (width, height and spacing, see Fig. 1), tool dimensions and location, and roller dimensions (diameter and length). After that, the raw gravure cylinder without specified pattern is installed on the machine, and outer diameter turning is conducted using the round nose diamond tool on the cylinder surface to achieve mirror surface quality with surface roughness less than 6 nm ($R_a$). Then, according to the generated CNC tool path program, DME is conducted to engrave the designed gravure pattern at specified positions on the roller surface. Finally, the machined gravure cylinder is measured to evaluate quality of the engraved pattern and consistency of the cell size and structure. Several iterations may be necessary to per-

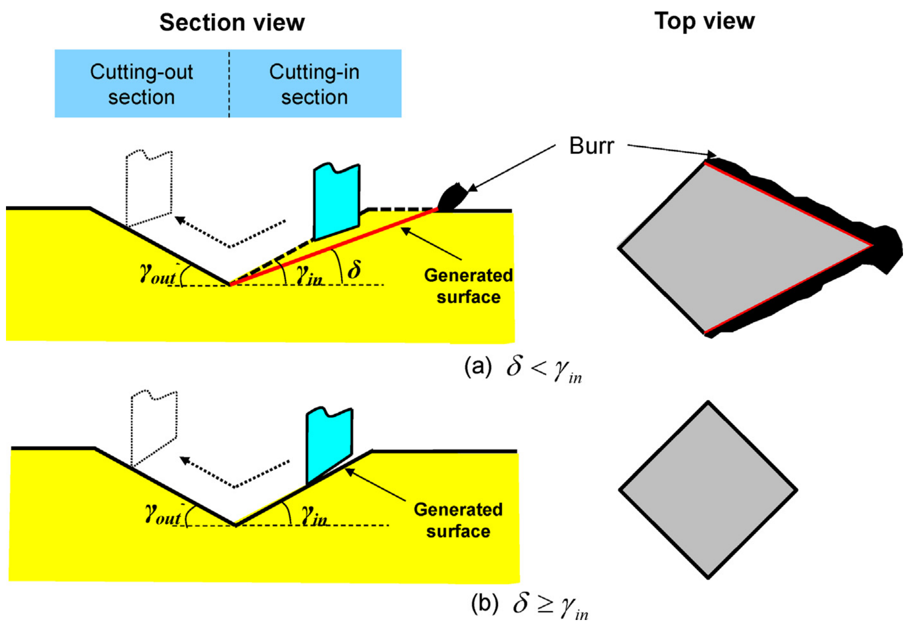


**Fig. 4.** Effects of the diamond tool clearance angle on cell generation and burr formation in the DME process.

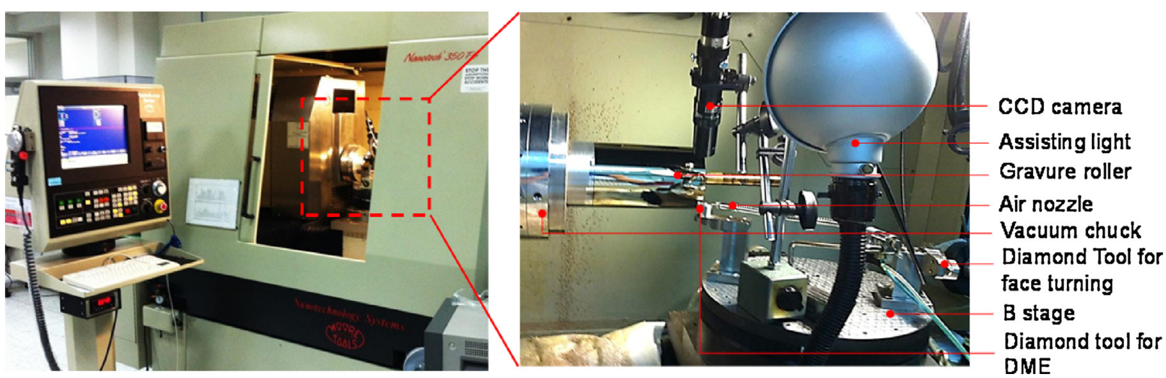


**Fig. 5.** Experimental setup for DME of a gravure roller.

form error compensation with updated CNC tool path program, in order to deliver the qualified gravure roller (see Fig. 6).

Table 1 shows details of the gravure roller, the gravure pattern and cell, and the machining conditions used in the experimental test. In gravure printing of electronics, the aspect ratio of gravure cells ($h/w$) is usually set as 0.4 or above, in order to ensure that enough volume of ink is transferred from the cells onto the film substrates and merges into continuous metal lines. According to Eqs. (1) and (3), the tool included angle should be smaller than or equal to 120°, and the cut-in and cut-out angles should be greater than or equal to 30°. The clearance angle is set to be equal to the cut-in angle to avoid interference between machined cell surface and the clearance face, and meanwhile to maintain the tool's robustness. The cell volume $V_c$ and aspect ratio are calculated as follows:

$$V_c = \frac{1}{3} w^2 h \quad (6)$$

### 3.2. Miniaturization of cell size

The mesh pattern and engraved cells on the machined roller are inspected using an optical microscope as well as a scanning electron microscope (SEM). As an example, Fig. 7 shows images of the gravure roller, the captured mesh pattern, and the engraved cells, which are taken by camera, microscope and SEM, respectively. From Fig. 7(a), it can be observed that mirror surface has been achieved on the non-patterned area with good reflection quality. Consistent cell size and mesh pattern can be observed from Fig. 7(b) and (c). From Fig. 7(d), the concave inverted pyramid structure of the engraved cell can be clearly observed. The zigzag profile on the engraved cell surface is caused by the Slow Slide Servo technique used to generate the interactive motion of the three machine axes, which are not purely linearly interpolated. This effect can be mini-

**Table 1**
Specifications of the gravure roller, mesh pattern, cell structure and cutting tool.

| | | |
|---|---|---|
| Gravure roller | Material | Brass |
| | Length | 150 mm |
| | Diameter | 100 mm |
| Mesh pattern & Cell structure | Mesh width | 305 μm |
| | Cell width | 7–32 μm |
| | Cell spacing | 1–5 μm |
| | Cell height | 2.8–12.8 μm |
| | Cell volume | 46–4369 fL |
| | Cell aspect ratio | 0.4 |
| Cutting tool | Material | Natural single crystal diamond |
| | Included angle | 120° |
| | Nose radius | <1 μm |
| | Rake angle | 0° |
| | Clearance angle | 30° |

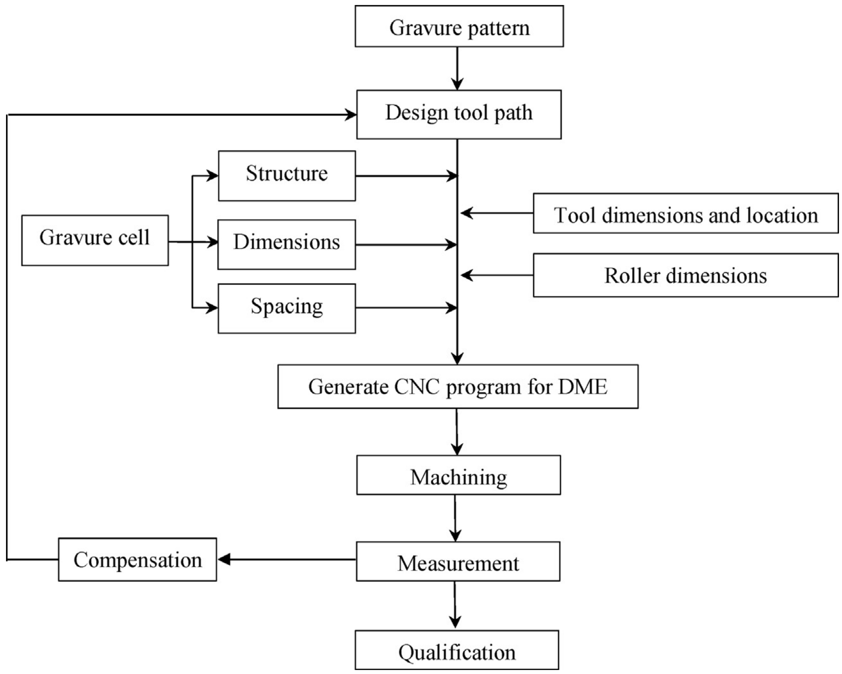


**Fig. 6.** Process flowchart for the proposed DME process.

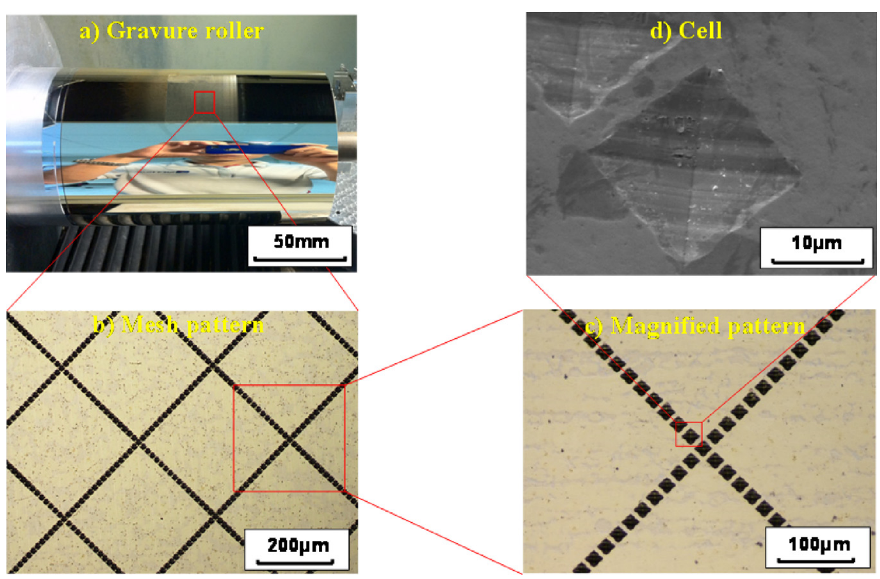


**Fig. 7.** Camera, microscope and SEM images of roller, mesh pattern ($50 \times 50\,\text{mm}^2$) and cells (18 μm width) machined by DME.

mized by increasing the resolution of programming points per unit cycle when generating the tool path.

By employing the proposed DME process, it is easier to realize cell size miniaturization than the other conventional engraving techniques. In this study, efforts are spent in miniaturizing the engraved gravure cells by reducing the engraving depth and meanwhile maintaining the consistence of cell structure and avoid the burr formation. Fig. 8 shows a series of gravure cells ranging from 32 μm to 7 μm which are machined by DME. In contrast, the smallest cell size which market-available gravure rollers could achieve is 25 μm by laser engraving. Some gravure roller manufacturers may claim their capability of engraving sub-20 μm gravure cells, but the generated gravure cells usually have inconsistent cell structure or size, which will result into varying ink volume transfer and hence uneven printed feature size in gravure printing of electronics.

The yet smallest cell width with consistent cell structure and burr-free profile achieved by DME using the 120° diamond tool on this brass roller is 7 μm, as shown in the left-most picture of Fig. 8. The minimum structure size which can be generated by DME is limited by a number of physical, technological and economic factors. Size effects, material swelling and recovery will become more obvious when the material removal rate is smaller than a certain value in micro machining process, which depends on the material properties, the tool edge radius and other cutting conditions. Hence, there is still great potential to continuously scale down the cell structure size to 5 μm or even less using the DME technique. But more influencing factors need to be considered in order to generate burr-free cells on gravure roller with consistent cell structure and size, such as diamond tool structure, cutting speed, and the fitting accuracy of three-axis tool trajectory.

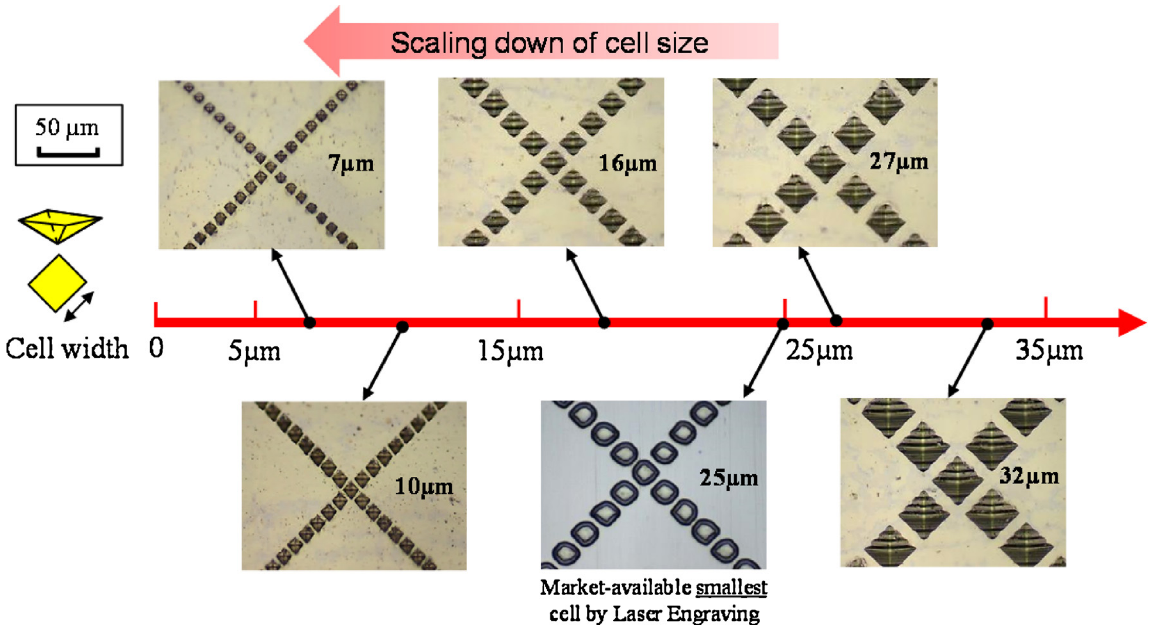


**Fig. 8.** Miniaturization of gravure cell size by DME.

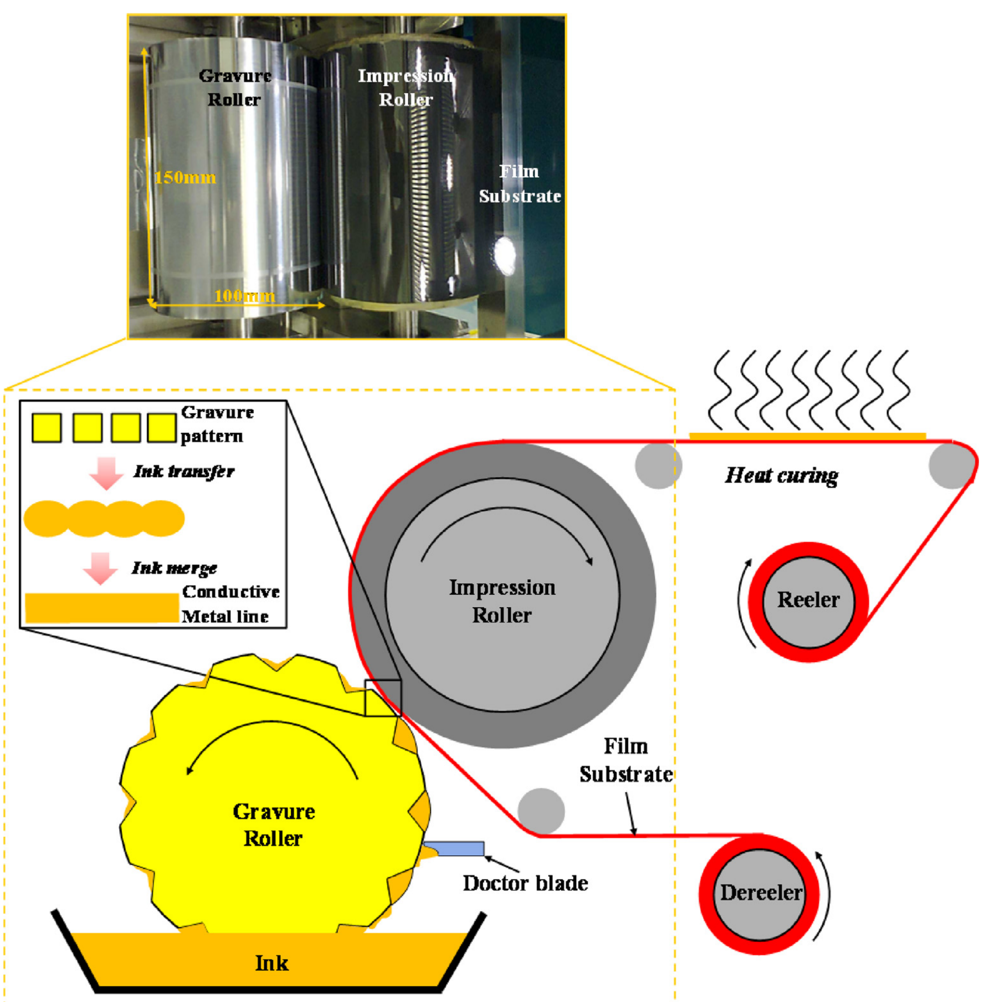


**Fig. 9.** Schematic process for gravure printing of electronics.

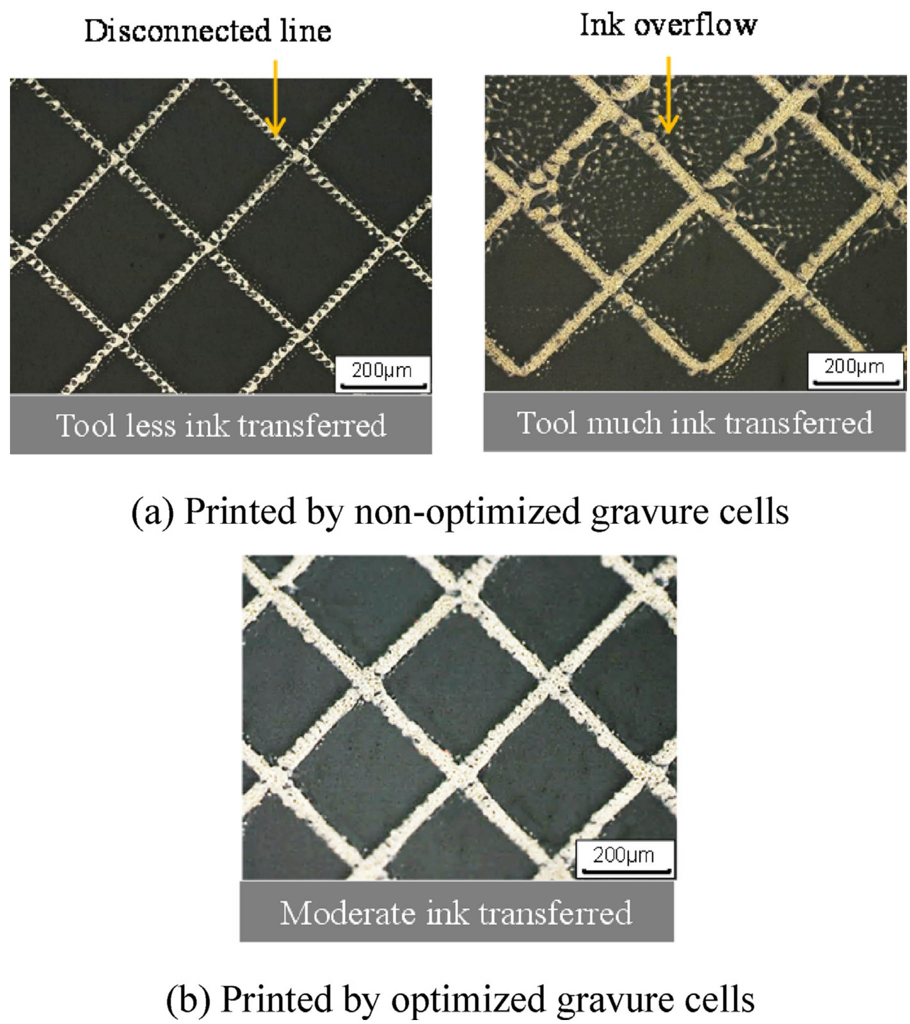


**Fig. 10.** Printed metal mesh by (a) non-optimized and (b) optimized gravure cell spacing.

## 4. Gravure printing of metal mesh using fabricated gravure rollers

### 4.1. Gravure printing of electronics

After demonstrating the capability of scaling down of gravure cell size using DME, several printing tests were conducted to evaluate the performance of engraved gravure rollers in printing the metal mesh TCF. Fig. 9 shows a schematic of R2R gravure printing of electronics on film substrate. The brass gravure roller with the micro engraved pattern is plated with a certain thickness (2–3 $\mu$m) of protective chrome layer. Then it is submerged in a pool filled with conductive nanoparticle ink. A raw film roll is installed on a motorized roller at the de-reeler station, which feeds the film substrate into the impression module at a web speed of 4 m/min. The ink is a solvent-based mixture made of silver nanoparticles (20–50 nm) with a given viscosity of 1000cp and a metal content of 10%. The film substrate is made of PET with a thickness of 100 $\mu$m. A doctor blade is tightly pressed on the gravure roller to wipe off excessive ink from non-patterned areas of the roller surface before they contact with the substrate. Depending on its cell volume, each cell will carry the particular amount of ink and place individual drops on the substrate after the gravure cell area contact with the impression roller. After the pattern is replicated from the gravure roller by transferring the liquid ink onto the film substrate, the ink is then cured by heat to evaporate the solvent and exsiccate the patterned film. During this curing process, the silver nanoparticles are bound together and tightly stick to the film substrate. Finally, the patterned film substrate is received by another motorized roller at the reeler.

### 4.2. Optimization of ink volume transfer

The ink volume transfer is affected by a number of factors which are mainly from the gravure cell parameters, gravure printing conditions, and properties of conductive ink. Cell spacing is a key parameter which determines the average ink volume transferred onto the film substrate per unit length, and hence the quality of the printed metal lines. If too much ink is transferred on the film, the excess ink will overflow to the non-patterned area and cause smearing and stain on the film, which could not only reduce the transmittance of the printed film, but may also induce short circuit between adjacent metal lines. If too little ink is transferred, the continuous metal lines cannot be formed, and a large number of pinholes will be found on the printed lines. This could significantly increase resistance of the printed electronics and even produce open circuits. An optimized value of cell spacing should realize moderate amount of ink transfer, which spreads and connects properly to form uniform and continuous metal lines. Fig. 10 shows a comparison between printed metal mesh with non-optimized and

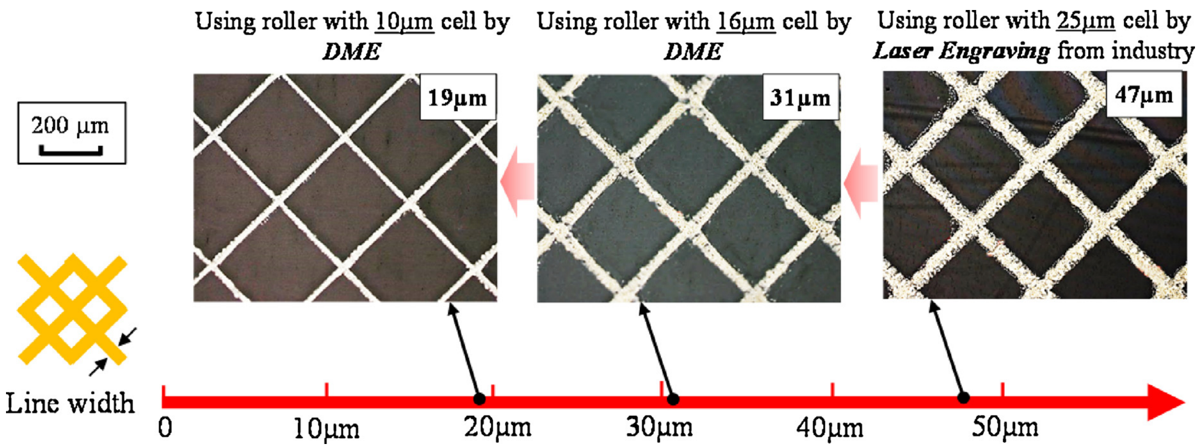


**Fig. 11.** Scaling down of printed line width using gravure rollers machined by DME.

optimized cell spacing. The gravure pattern in Fig. 10(b) has a cell width of 15 μm, and its other relevant parameters can be found in Table 1.

### 4.3. Scaling down of printed line width

Fig. 11 shows three microscope images of printed metal mesh using a market-available gravure roller machined by laser engraving (25 μm cell width) and two rollers machined by DME (16 μm and 10 μm cell width). It can be observed that the laser-engraved roller (25 μm cell width) provides the widest printed metal lines. Using the rollers engraved by DME with smaller cell width, the printed line width can be continuously reduced. Finally, metal mesh with consistent 19 μm line width is achieved with no ink overflow or broken lines. It is necessary to note that, besides applying smaller gravure cells, researchers (Kitsomboonloha et al., 2012; Sung et al., 2010) have also found that the printed line width can be further scaled down by improving the printing process from other aspects, such as using finer nanoparticle ink, optimizing the printing parameters (e.g. increasing the printing speed), redesigning the doctor blade, etc.

Transmittance with respect to visible light is an important feature of transparent conductive film used in touch screen modules. Its value should be at least greater than 80% to allow enough light passing through the film. Transmittance of the metal mesh is mainly determined by the covering percentage of non-patterned area which allows the light to pass through. In this study, the transmittance of the printed films is measured using a UV–vis Spectrophotometer, and the results are shown in Fig. 12. When the line width is decreased from 47 μm to 19 μm, the average transmittance of printed metal mesh film in the visible light region (390–700 nm) is increased from 65.2% to 80.4%, which is comparable to the transmittance of ITO transparent conductive film (typically ≥80%). These results have successfully proven the feasibility of using printed metal mesh to replace ITO in the near future.

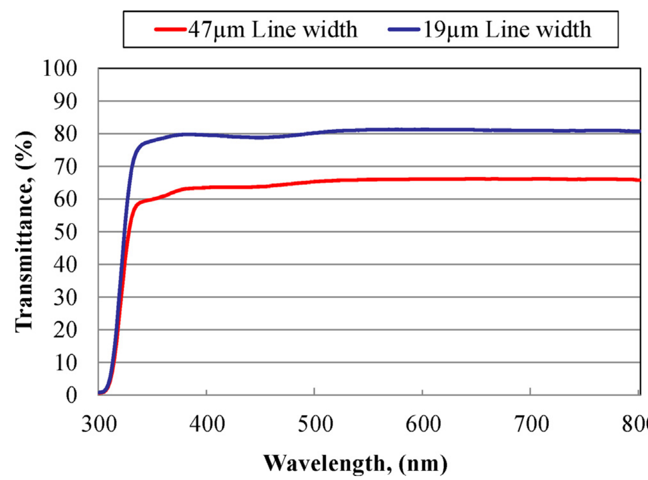


**Fig. 12.** Transmittance of metal mesh films printed using rollers engraved by DME (19 μm line width) and conventional laser engraving (47 μm line width).

## 5. Summary and outlook

In this paper, Diamond Micro Engraving, a novel method to realize engraving of high-precision gravure roller based on ultraprecision machining technology, has been introduced. By employing DME, cell size miniaturization on gravure roller moulds is achieved, which accordingly scales down the feature width of printed metal lines in roll-to-roll gravure printing of electronics (e.g. metal mesh). Based on the results, conclusions can be compiled as follows:

- Gravure cells with concave inverted pyramid structure on metal rollers is able to be continuously machined using a V-shape sharp-nose diamond tool by employing the Slow Slide Servo technology on the ultraprecision machining system.
- The width of micro engraved gravure cells is successfully miniaturized to 7 μm with consistent cell structure and size by applying the proposed DME process, which is a significant improvement over the industry norm of 25 μm obtained by laser engraving.
- By replacing the laser-engraved roller with the gravure rollers machined by DME, the line width of printed metal mesh film, which works as a kind of transparent conductive film used in touch screen modules, is reduced from 47 μm to 19 μm, and its transmittance for visible light is increased from 65.2% to 80.4%.
- DME is an industry-feasible technique based on existing ultraprecision machining technology, and there are no obvious barriers to stop researchers and engineers to apply this process to fabricate gravure rollers patterned with miniaturized cells for high-performance electronics printing.

The potential of the DME process was demonstrated in this study. However, additional research should be conducted in order to further reduce the cell size, and to increase the machining speed by applying the Fast Tool Servo (FTS) technology.

## References

Brinksmeier, E., Schönemann, L., 2014. Generation of discontinuous microstructures by diamond micro chiseling. CIRP Ann. 63 (1), 49–52.

Brinksmeier, E., Gläbe, R., Schönemann, L., 2012a. Diamond micro chiseling of large-scale retroreflective arrays. Precis. Eng. 36, 650–657.

Brinksmeier, E., Gläbe, R., Schönemann, L., 2012b. Review on diamond-machining processes for the generation of functional surface structures. CIRP J. Manuf. Sci. Technol. 5, 1–7.

Donaldson, R., Patterson, S., 1983. Design and construction of a large, vertical axis diamond turning machine. In: 27th Annual Techincal Symposium, International Society for Optics and Photonics, pp. 62–67.

Hrehorova, E., Rebros, M., Pekarovicova, A., Bazuin, B., Ranganathan, A., Garner, S., Merz, G., Tosch, J., Boudreau, R., 2011. Gravure printing of conductive inks on glass substrates for applications in printed electronics. Display Technol. J. 7, 318–324.

Kang, H., Kitsomboonloha, R., Jang, J., Subramanian, V., 2012. High-performance printed transistors realized using femtoliter gravure-printed sub-10m metallic nanoparticle patterns and highly uniform polymer dielectric and semiconductor layers. Adv. Mater. 24, 3065–3069.

Kitsomboonloha, R., Morris, S., Rong, X., Subramanian, V., 2012. Femtoliter-scale patterning by high-speed, highly scaled inverse gravure printing. Langmuir 28, 16711–16723.

Pudas, M., Halonen, N., Granat, P., Vähäkangas, J., 2005. Gravure printing of conductive particulate polymer inks on flexible substrates. Prog. Org. Coat. 54, 310–316.printing.Sung, D., de la Fuente Vornbrock, A., Subramanian, V., 2010. Scaling and optimization of gravure-printed silver nanoparticle lines for printed electronics. Componen. Packag. Technol. IEEE Trans. 33, 105–114.

Tvingstedt, K., Inganäs, O., 2007. Electrode grids for ITO free organic photovoltaic devices. Adv. Mater. 19, 2893–2897.